The 2010 IEEE/RSJ International Conference on
Intelligent Robots and Systems
October 18-22, 2010, Taipei, Taiwan

Fault Tolerance Measurement Using a Six-Axis Force/Torque Sensing System with Redundancy

Toshiaki Tsuji and Ryosuke Hanyu

Abstract— **Force sensors are a useful tool for robot adapting to human environments. However, these sensors are rarely used for commercial machines requiring safety since it is difficult to eliminate the possibility of failure. Although fault tolerance is an important issue, no critical method for general force measurement is proposed in the past. Hence, this paper proposes a fault tolerance measurement method using sensing devices with redundancy. The proposed method accomplishes both: fault detection without additional sensors; and force estimation during fault period. Furthermore, the fault detection handles many kinds of faults such as disconnection of wires, peeling of strain gauge, and so on. The validity of the proposed method is verified through some simulations and experiments.**

I. INTRODUCTION

Robots are highly expected to work in the real environments and support human in the near future. However, still some issues remain. How robots adapt to the human environment is one of the most important issues. One approach for the issue is an environment recognition system using image sensors, which is currently being studied by a large number of researchers [1], [2], [3]. Force information is also an inevitable factor since robots always have some physical interaction with human and environment. Robots are required to recognize its environment based on force information for adaptation to the real environment. For example, Morisawa and Ohnishi achieved advanced behavior in a biped humanoid robot to adapt to changes in its environment by recognizing the floor surface as reduced-order environmental mode variables [4]. Function-based control is also a good candidate for environment recognition based on force information in space domain [5]. Another example is a robot, which can recognize the shape of a grasped object, using the response values of tactile sensors [6]. Force information is important not only for environment recognition but also for collision mitigation or shock absorption if the robot runs into a person or some objects in the surrounding environment, and many collision mitigation control methods for robots using force sensors have been proposed. Supposing that any part of the robot can come into contact with a person or object in the environment, whole-body force sensation technology is inevitable for collision mitigation control [7], [8]. Some studies have shown that the sensing region can be expanded by applying force sensors. Salisbury proposed a tactile sensing method that identifies contact features on an insensitive end-effector using a six-axis force sensor [9]. Here, the contact features are: a) the contact location and b) the magnitude and direction of the contact force. Bicchi has proposed an idea of intrinsic contact sensing that identifies the contact features in elastic robot fingers [10].

Although force sensors are a useful tool for robot adapting to human environments, these sensors are rarely used for commercial machines requiring safety since it is difficult to eliminate the possibility of failure. Most of force sensors may fail by impact. Disconnection and contact failure on wires are also often causing failure. The faulty force sensors are extremely dangerous since it may make the control system unstable.

For solving the issue, fault tolerant control is quite popular [11], [12], [13] while there are only a few studies dealing with force sensors. Yubai, et al. have achieved fault detection and fault tolerance control using an external force estimation observer [14]. The method still has an issue that unmeasurable force axes often exist since dimension of force detection is limited by the number of actuators. On the other hand, Hosoda, et al. demonstrated that fault tolerance in the detection of external force could be improved using a sensor integrating a large number of sensor devices embedded in a soft fingertip [15], but the object must be a soft end-effector in this case.

Although fault tolerance is an important issue, no critical method for general force measurement is proposed in the past. Some examples of practical solutions exist in industry while they require duplexed sensors for fault detection. Furthermore, a generalized method for force estimation during fault is not shown yet. Therefore, this paper proposes a fault tolerance measurement method using sensing devices with redundancy. A 6-axis force/torque sensing system with 9-channel redundancy consisting of a combined device of three 3-axis force sensors is developed. The system measures external force by integrating the response values of the combined sensors. It then estimates the correct 6-axis force/torque information based on the values received from the sensors other than the faulty one. The estimation method is an extension of the idea of principal component analysis [16]. Since no common-type force/torque sensors accomplish both fault detection and external force estimation at the same time, it is expected that the proposed method will solve the safety issue due to failure of force sensors, which is an essential problem to be solved for human support robots.

This work was supported in part by PRESTO grant from Japan Science and Technology Agency(JST).

T. Tsuji is with Department of Electrical and Electronic Systems, Faculty of Engineering, Saitama University. He is also a JST PRESTO researcher. tsuji@ees.saitama-u.ac.jp

R. Hanyu is with Department of Electrical and Electronic Systems, Faculty of Engineering, Saitama University

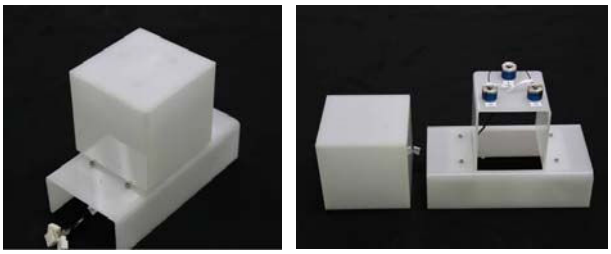

Fig. 1. Experimental setup

II. Configuration of Proposed Force Sensing System

Fig. 1 shows the force/torque sensing system proposed in this study. This system has been developed as a prototype the Haptic Armor[17], which is a whole-body force sensation sensor, consisting of a shell-shaped end-effector composed of acrylic board and a device with three 3-axis force/torque sensors that support the end-effector. Each force sensor supports the end-effector on a small contact area so that a point contact between the force sensor and the end-effector can be assumed.

The sensor system can be used as a tactile-sensing mechanism to measure the position that external force is applied. In this study, however, it is used as a 6-axis force/torque sensing system that measures the 3-axis external forces and moments generated in the end-effector. Shown below are the computational algorithms used for measurement of the external forces and moments.

Given the sum of external forces and moments generated in the sensor's end-effector, expressed as $\boldsymbol{F}^e$ and $\boldsymbol{M}^e$, respectively, the equilibrium of the force and moment acting on the end-effector can be calculated by the following expressions, respectively:

$$\boldsymbol{F}^e + \sum_{i=1}^{m} \boldsymbol{F}_i^s = \boldsymbol{0} \tag{1}$$

$$\boldsymbol{M}^e + \sum_{i=1}^{m} \boldsymbol{F}_i^s \times (\boldsymbol{P}_i^s - \boldsymbol{P}^o) = \boldsymbol{0} \tag{2}$$

where $\boldsymbol{F}_i^s$ is the force to be generated at the ith support point that, ideally speaking, conforms to the sensor output although the sensor output value vector is the reverse of $\boldsymbol{F}_i^s$ because of the action-reaction relationship; $\boldsymbol{P}^o$ represents the normal coordinates of the external force moment, and $\boldsymbol{P}_i^s$ represents the coordinates of the ith support point. m is the number of 3-axis force/torque sensors that support the end-effector, which is three in this paper. (Fig. 1)

Equations (1) and (2) above can be combined as follows:

$$\boldsymbol{\Gamma} = \boldsymbol{T}\boldsymbol{F}^d \tag{3}$$

$$\boldsymbol{\Gamma} = \begin{bmatrix} \boldsymbol{F}^e \\ \boldsymbol{M}^e \end{bmatrix},$$

$$\boldsymbol{T} = \begin{bmatrix} \boldsymbol{I}_3 & \boldsymbol{I}_3 & \cdots & \boldsymbol{I}_3 \\ \boldsymbol{t}_1^p & \boldsymbol{t}_2^p & \cdots & \boldsymbol{t}_m^p \end{bmatrix},$$

$$\boldsymbol{F}^d = \begin{bmatrix} -\boldsymbol{F}_1^s \\ -\boldsymbol{F}_2^s \\ \vdots \\ -\boldsymbol{F}_m^s \end{bmatrix}.$$

Here, $\boldsymbol{t}_i^p$ is a skew-symmetric matrix for calculating the outer product of vectors $(\boldsymbol{P_i^s} - \boldsymbol{P}^o)$ and is given by the following expression:

$$\boldsymbol{t}_i^p = \begin{bmatrix} 0 & P_{iz}^s - P_z^o & -P_{iy}^s + P_y^o \\ -P_{iz}^s + P_z^o & 0 & P_{ix}^s - P_x^o \\ P_{iy}^s - P_y^o & -P_{ix}^s + P_x^o & 0 \end{bmatrix}.$$

Equation (3) is the formula for linear mapping of the $3m$-dimensional vector space, comprising sensor response value vectors $\boldsymbol{F}^d$, to the six-dimensional force/moment space.

III. Fault Tolerance Algorithm

A. Basic Concept

Essentially, sensor response value vectors $\boldsymbol{F}^d$ can be any value in the vector space corresponding to the external force values. However, where multiple sensors support a rigid end-effector having fewer degrees of freedom than the number of sensor channels, as in this study, the end-effector mechanism restrains the force/torque sensors, and thus limits the sensor response value vectors to reduced-order dimensions. Where sensor response values are determined in a one-to-one manner proportional to the six-dimensional external force patterns to be generated in the end-effector, the aggregate of their vectors is present on the six-dimensional hyper plane within the $3m$-dimensional vector space as shown in Fig. 2. If there is no sensor response value vector on this hyper plane, it indicates that a value not meeting the restraining conditions of the end-effector mechanism has been output, thus providing a warning that an incorrect wrong value is being output from one of the sensors. Fault detection and localization is performed by paying attention to this characteristic.

B. Fault Detection

To begin with, sensor response value vectors $\boldsymbol{F}^d$ are in principle determined by the following expression in a one-to-one manner proportional to the six-dimensional external force patterns:

$$\boldsymbol{F}^d = \boldsymbol{T}^{inv}\boldsymbol{\Gamma} \tag{4}$$

where $\boldsymbol{T}^{inv}$ is the inverse transformation matrix of $\boldsymbol{T}$ and acts to restrain $\boldsymbol{F}^d$ on the six-dimensional hyper plane. As the number of dimensions of vectors $\boldsymbol{F}^d$ is greater than six and $\boldsymbol{T}$ does not become a nonsingular matrix, inverse transformation matrix $\boldsymbol{T}^{inv}$ cannot be uniquely determined. Also, the value of $\boldsymbol{T}^{inv}$ depends on the internal force and other factors present at the time when the end-effector is secured by each force/torque sensor. Therefore, to derive $\boldsymbol{T}^{inv}$, experimental data for calibration must be obtained after securing the end-effector.

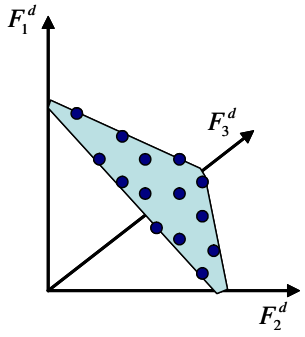

Fig. 2. Hyperplane in sensor space

Accordingly, to obtain the data for calibration, an experiment is conducted in which n types of different known external forces are applied. If the ith external force vector is represented by $\mathbf{\Gamma}_i$, the external force data for calibration can be given by the following:

$$\mathbf{\Gamma}_a = \begin{bmatrix} \mathbf{\Gamma}_1 & \mathbf{\Gamma}_2 & \cdots & \mathbf{\Gamma}_n \end{bmatrix} \tag{5}$$

Then, the following are formulated:

$$\boldsymbol{F}_a^d = \boldsymbol{T}^{inv}\mathbf{\Gamma}_a \tag{6}$$

$$\boldsymbol{F}_a^d = \begin{bmatrix} \boldsymbol{F}_1^d & \boldsymbol{F}_2^d & \cdots & \boldsymbol{F}_n^d \end{bmatrix} \tag{7}$$

$\boldsymbol{F}_i^d$ is the sensor output when the ith external force is applied.

When six or more types of external forces are applied, inverse transformation matrix $\boldsymbol{T}^{inv}$ can be derived using the resulting data and (8):

$$\begin{aligned} \boldsymbol{T}^{inv} &= \boldsymbol{F}_a^d\mathbf{\Gamma}_a^+ \\ \mathbf{\Gamma}_a^+ &= \mathbf{\Gamma}_a^T(\mathbf{\Gamma}_a\mathbf{\Gamma}_a^T)^{-1} \end{aligned} \tag{8}$$

Due to the nature of a pseudo-inverse matrix, the matrix obtained from (8) is the least square approximation solution of the measured value. Therefore, the calculation accuracy for $\boldsymbol{T}^{inv}$ can be improved by increasing the number n of external force patterns to obtain a larger volume of data for calibration. The calibration experiment is conducted based on the theory described above, and fault detection is implemented using the inverse transformation matrix $\boldsymbol{T}^{inv}$ previously derived. As described earlier, $\boldsymbol{F}^d$ is in theory restrained on the six-dimensional hyper plane and its ideal value $\boldsymbol{F}^i$ is derived by the following expression:

$$\begin{aligned} \boldsymbol{F}^i &= \boldsymbol{T}^{inv}\mathbf{\Gamma} \\ &= \boldsymbol{T}^{inv}\boldsymbol{T}\boldsymbol{F}^d \end{aligned} \tag{9}$$

In practice, however, a deviation $\boldsymbol{F}^f$ from the ideal value is caused due to various types of errors:

$$\boldsymbol{F}^f = \boldsymbol{F}^d - \boldsymbol{F}^i \tag{10}$$

Substituting (10) with (9), gives Expression (11):

$$\begin{aligned} \boldsymbol{F}^f &= (\boldsymbol{I} - \boldsymbol{T}^{inv}\boldsymbol{T})\boldsymbol{F}^d \\ &= \boldsymbol{Q}\boldsymbol{F}^d \end{aligned} \tag{11}$$

where,

$$\begin{aligned} \boldsymbol{Q} &= \boldsymbol{I} - \boldsymbol{T}^{inv}\boldsymbol{T} \\ &= \begin{bmatrix} \boldsymbol{q}_1 & \boldsymbol{q}_2 & \cdots & \boldsymbol{q}_{3m} \end{bmatrix} \end{aligned}$$

Ideally speaking, $\boldsymbol{F}^f$ is always a zero vector when a proper sensor response $\boldsymbol{F}^d$ is acquired. If an error is implied in the value $\boldsymbol{F}^d$, it deviates from the six-dimensional hyper plane, and thus the value $\boldsymbol{F}^f$ will become larger. In particular, if an incorrect value is output from a specific jth channel due to the sensor failure, $\boldsymbol{F}^f$ should be almost proportional to $\boldsymbol{q}_j$, the jth column in $\boldsymbol{Q}$. This means that sensor fault detection and localization can be performed by checking the inner product of $\boldsymbol{F}^f$ and $\boldsymbol{q}_j$. If $\boldsymbol{F}^f \cdot \boldsymbol{q}_j$ is the largest of all innner products and the value exceeds the threshold, the jth channel is identified as failure. The threshold should be determined from the maximum sensor noise detected during experiments without failure.

C. Force Estimation during Fault

Next, we propose a sensor response estimation method to ensure reliable performance of the proposed 6-axis force/torque sensing system during failure. If the point of fault has been localized by the method described above, the sensor response value at the faulty point is substituted by its theoretical value $\boldsymbol{F}^i$ to obtain an estimated value $\boldsymbol{F}^c$. Sensor response values are applicable to other elements. Nevertheless, the theoretical value $\boldsymbol{F}^i$ is not always correct because it has been calculated based on $\boldsymbol{F}^d$, which contains errors caused by the failure.

From the inner product value derived above, it is possible to estimate the error of the fault sensor channel. The compensated response $\boldsymbol{F}^c$ is derived by the following equation.

$$\boldsymbol{F}^c = \begin{bmatrix} F_1^d \\ \vdots \\ F_j^d - \dfrac{\boldsymbol{F}^f \cdot \boldsymbol{q}_j}{|\boldsymbol{q}_j|} \\ \vdots \\ F_{3m}^d \end{bmatrix} \tag{12}$$

D. Aspect of the Method

In sum, the proposed method accomplishes following factors:

- fault detection without additional sensors
- force estimation during fault period.

The proposed method is the only method that accomplishes both at the same time. Furthermore, the fault detection handles many kinds of faults such as disconnection of wires, peeling of strain gauge, and so on.

There is an exceptioin that $\boldsymbol{F}^d$ still remains on the six-dimensional hyper plane. Then the fault is not detected. The exception occurs when colums in $\mathbf{\Gamma}_a$ are linearly dependent. Hence, the condition to avoid undetection of fault is to calibrate the sensor by independent force vectors.

For fault detection, the number of force sensing channels should be larger than the DOF of force/torque measurement.

If the channel number exceeds measurement DOF more than 2, fault detection works with high-reliability. On the other hand, identification of faulty channel sometimes failed when the channel number exceeds measurement DOF only 1.

Although this study uses a multi support mechanism with 3 force sensors, it is also applicable to a force sensor unit with redundant channels of strain measurement.

IV. Simulations

This section presents the results obtained from simulations conducted to verify the proposed algorithms. Another purpose of the simulation is to verify the error from the true value, which cannot be measured in experiments. The simulation models used for the purposes are shown in Fig. 3. Here, the simulations are performed on a two-dimensional plane for simplification. In the model structure, a circular end-effector is supported by three 2-axis force sensors. The three force sensors are fixed to the center base and are used for measurement of forces in the $x-/y-$axis directions.

The end-effector moves slightly in the $x-/y-$axis directions as well as in its rotating direction and therefore can be utilized as a 3-axis force/torque sensor. Its angle of rotation is θ. A total of six channels (2-axis$\times$3) can be measured by this end-effector, and it has a redundancy corresponding to three degrees of freedom. The end-effector is deemed to be a rigid body, and the supporting force/torque sensors are deemed to be springs of high rigidity, provided, however, that these springs count on rigidity k in the $x-/y-$axis directions, respectively, and that no moment is produced around the contact between the end-effector and springs.

Shown in Fig. 4 are the results obtained when external forces $F_x^e = 1.0 \times \sin(t)$, $F_y^e = 1.0 \times \cos(1.3t)$, $M_\theta^e = 0.1 \times \sin(0.1t)$ were applied. Note, however, that incorrect sensor response values as shown below were output to simulate faults:

$$
\begin{aligned}
F_{1y}^d &= 0.0, (5 < t < 8) \\
F_{2x}^d &= 5.0, (10 < t < 13) \\
F_{2y}^d &= -5.0, (15 < t < 18) \\
F_{3x}^d &= 0.4, (20 < t < 23) \\
F_{3y}^d &= 0.4, (25 < t < 28)
\end{aligned}
$$

Both the external force response value and the estimated value agree with the true value when the sensors are sound. On the other hand, it can be seen that the deviation between the response value and the true value increases when a fault occurs. It was verified that at that time (when a fault arose) the estimated value remained practically without errors, following the true value, thus proving that the proposed external force estimation algorithm at failure works satisfactorily, excluding the following exceptional case: it was confirmed that an error of about 0.1 N was contained in the estimated value for 20-23 s. The fault input given at that time scarcely involved a deviation from the actual response value, not suggesting a failure, and the sensor response value was used as is as the estimated value; that is, if a failure arises involving a very small error of almost unrecognizable scale, then a very small error proportional to such scale will remain.

TABLE I

Specifications of the simulation model

Stiffness of force sensors	900	[N/m]
Damping factor of force sensors	10	[N/m]
Weight of end-effector	0.2	[kg]
Radius of end-effector	0.12	[m]
Threshold of sensor error	0.1	[N]

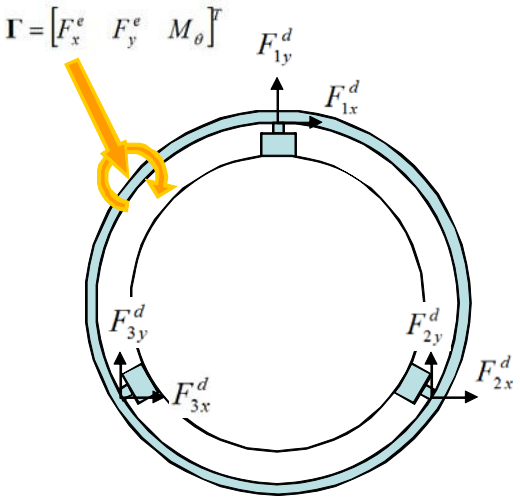

Fig. 3. Simulation model

V. Experiment

Experiments were conducted for verification of the proposed method in a practical system. Fig. 5 shows the experimental system. In the photo, a weight was put on the sensor and the detected force vector was displayed by an OpenGL program. Table II shows the specification of the force sensors used in this study.

Force measurement results are shown in Fig. 6. Fig. 6(a) shows the result when gravity force was applied vertically by a 1kg weight. On the other hand, Fig. 6(b) shows the result when gravity force was applied at an angle of about 20 degrees by tilting the force sensor. In both experiments, the 9 wires of force sensors were disconnected one by one. The shaded areas indicate the disconnected periods. The impulsive variations of force responses show the force measurement results when failures occurred. The error due to the failure converged to much smaller error in a short term. There was no big difference of the average and the maximum errors with the two experiments. In Fig. 6(a), the average RMS error of all faulty channels were 0.84N(8.8%) while the channel with maximum error produced 2.53N(26.4%) RMS error. Since the average error of the force sensor without any failure was 0.39N(4.1%), it can be said that the force estimation during failure was accomplished while some errors were produced. The results also show that the

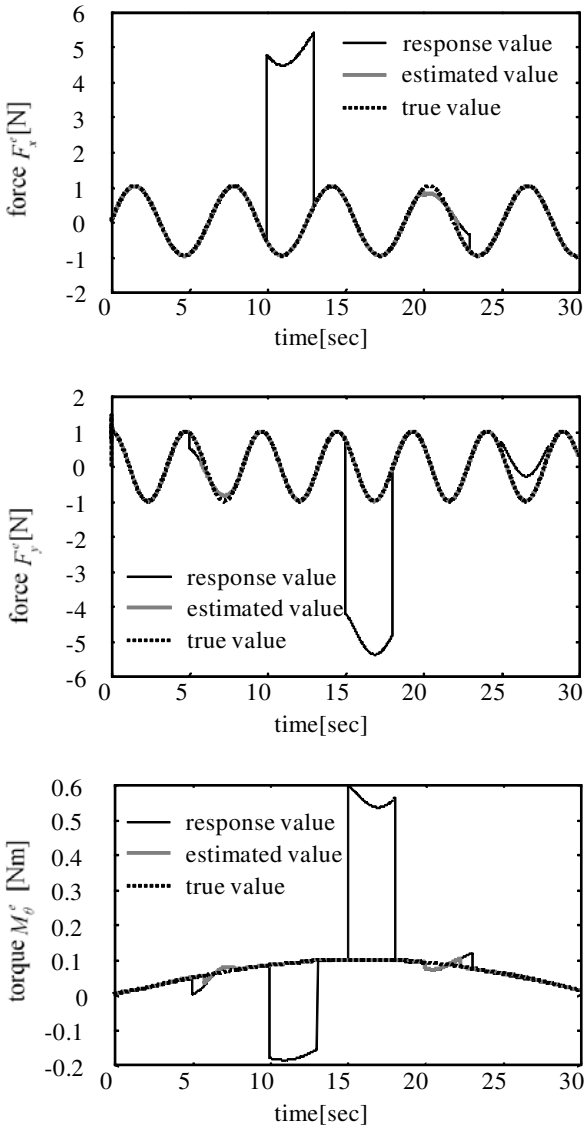

Fig. 4. Simulation result

error depends on the sensing direction. Since vertical force was applied to the sensor, large error was produced at the channel which detects vertical force. Hence arrangement of force sensors should be considered so that each force sensors detect different force direction.

Theoretically, the error due to fault can be recognized at the sample immediately after the fault. Hence the impulsive variation can be removed. The recognition delay due to sensor noise is the main issue here and our future works is to remove the impulsive variation by eliminating the recognition delay.

VI. Conclusion

This paper proposes a fault tolerance measurement method using sensing devices with redundancy. The proposed method accomplishes both: fault detection without additional sensors; and force estimation during fault period. Furthermore, the fault detection handles many kinds of faults such as disconnection of wires, peeling of strain gauge, and so on. Although this study used a model with three sensors arranged in a distributed manner for the verification process in this study, the proposed method can also be applied to a centralized-type sensor such as the common-type 6-axis force/torque sensor in which all sensor devices are mounted at a single point. Our future works are to deal with multiple fault occuring at the same time and to clarify the way of determining sensor arrangement.

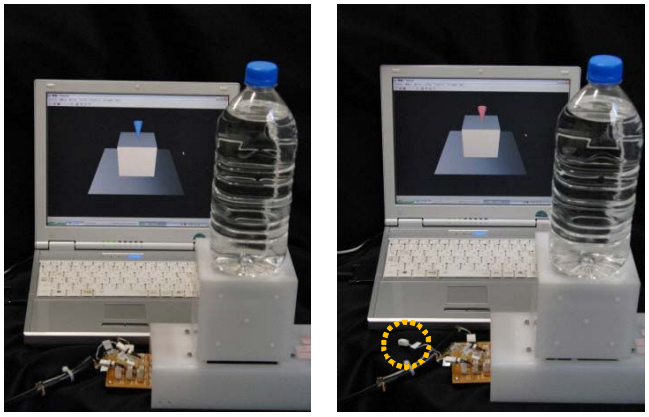

(a) Detected force vector without failure

(b) Estimated force vector during failure

Fig. 5. Photo of the experimental system

TABLE II
SPECIFICATIONS OF THE FORCE SENSOR

Maker	Nitta Co.
Type	PD3-32-10-15
Rated force	15 N
Sensing bandwidth	100Hz
Linearity error	2% of full scale or less
Hysteresis	2% of full scale or less
Sensitivity	500-900mV/FS
Weight	13 g

References

[1] R. T. Chin, C. R. Dyer: "Model-based recognition in robot vision," *ACM Computing Surveys*, Vol. 18, No. 1, pp. 67–108, 1986.

[2] I. Ishii, K. Yamamoto, and M. Kubozono: "Higher Order Autocorrelation Vision Chip," *IEEE Trans. on Electron Devices*, Vol. 53, No. 8, pp. 1797–1804, 2006.

[3] T. Tsuji: "Removal of Specular Reflection Light on High-speed Vision System," *Proc. IEEE Int. Conf. Robotics & Automation*, pp. 1542–1547, 2010.

[4] M. Morisawa, K. Ohnishi: "Motion Control Talking Environmental Information into Account," *EPE Journal*, Vol. 12, No. 4, pp. 37–41, 2002.

[5] T. Tsuji, K. Ohnishi, A. Sabanovic: "A Controller Design Method based on Functionality," *IEEE Trans. on Ind. Electron.* Vol. 54, No. 6, pp. 3335–3343, 2007.

[6] N. Furukawa, A. Namiki, T. Senoo, M. Ishikawa : "Dynamic Regrasping Using a High-speed Multifingered Hand and a High-speed Vision System", *Proc. IEEE Int. Conf. on Robotics & Automation*, pp.181–187, 2006.

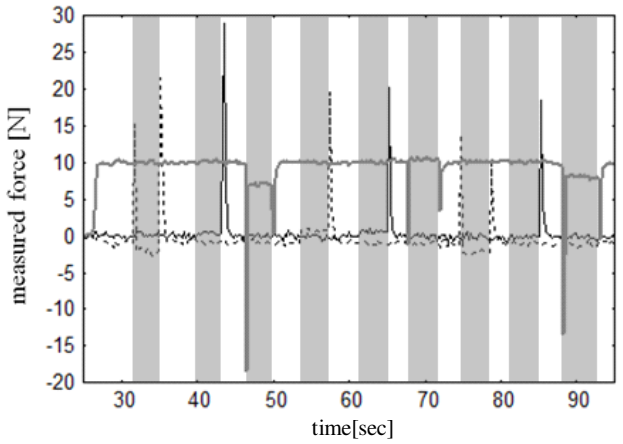

(a) When gravity force was applied vertically

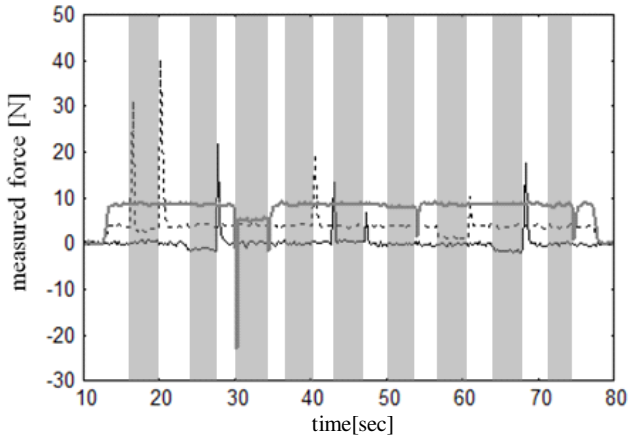

(b) When gravity force was applied at an angle

Fig. 6. Force response in experiment

[7] J. Urbano, K. Terashima, T. Miyoshi, H. Kitagawa: "Impedance control for safety and comfortable navigation of an omni-directional mobile wheelchair," *Proc. IEEE/RSJ Int. Conf. on Intelligent Robots and Systems*, vol.2, pp. 1902–1907, 2004

[8] Y. Shoji, M. Inaba and T. Fukuda: "Stable Contact Control of Robotic Manipulator Based on Unified Approach," *J. Robot. Soc. Jpn.*, Vol. 11, No. 5, pp. 77–91, 1993.

[9] J. Salisbury: "Interpretation of contact geometries from force measurements," *Proc. IEEE Int. Conf. Robotics & Automation*, pp. 240–247, 1984.

[10] A. Bicchi: "Intrinsic Contact Sensing for Soft Fingers," *Proc. IEEE Int. Conf. Robotics & Automation*, pp. 968–973, 1990.

[11] R. J. Patton: "Fault-tolerant control systems: The 1997 situation," *IFAC Safeprocess'97*, pp. 1033–1055.

[12] M. Sampath, R. Sengupta, S. Lafortune, K. Sinnamohideen, and D. C. Teneketzis: "Failure diagnosis using discrete-event models," *IEEE Trans. Control Systems Techn.*, Vol. 4, No. 2, 105–123, 1996.

[13] M. Blanke, R. Izadi-Zamanabadi, S. A. Bogh, and C. P. Lunau: "Fault-tolerant control systems – a holistic view," *Control Engineering Practice*, Vol. 5, No. 5, pp. 693–702, 1997.

[14] Y. Izumikawa, K. Yubai, and J. Hirai: "Fault-Tolerant Control System of Flexible Arm for Sensor Fault by Using Reaction Force Observer," *IEEE/ASME Trans. on Mechatronics*, Vol. 10, No. 4, pp. 391–396, 2005.

[15] S. Takamuku, A. Fukuda and K. Hosoda: "Repetitive Grasping with Anthropomorphic Skin-Covered Hand Enables Robust Haptic Recognition," *Proc. IEEE/RSJ Int. Conf. on Intelligent Robots and Systems*, ThAT13.5, 2008.

[16] R. Dunia, S. J. Qin, T. F. Edgar, T. J. McAvoy: "Use of Principal Component Analysis for Sensor Fault Identification," *Computers Chem. Engng.*, Vol. 20, pp. S713–718, 1996.

[17] T. Tsuji, Y. Kaneko, S. Abe: "Whole-body Force Sensation by Force Sensor with Shell-shaped End-effector," *IEEE Trans. Ind. Electron.*, Vol. 56, No. 5, pp. 1375–1382, 2009.

[18] T. Murakami, F. Yu, K. Ohnishi: "Torque Sensorless Control in Multidegree-of-Freedom Manipulator," *IEEE Trans. Ind. Electron.*, Vol. 40, No. 2, pp. 259–265, 1993.

[19] H. Iwata and S. Sugano: "Whole-body Covering Tactile Interface for Human Robot Coordination," *Proc. IEEE Int. Conf. Robotics & Automation*, pp. 3818–3824, 2002.

[20] K. Kamiyama, K. Vlack, T. Mizota, H. Kajimoto, N. Kawakami, S. Tachi: "Vision-Based Sensor for Real-Time Measuring of Surface Traction Fields," *IEEE Computer Graphics & Applications Magazine*, Vol. Jan-Feb 2005, pp.68–75, 2005.

[21] T. Tsuji, H. Nishi and K. Ohnishi: "A Controller Design Method of Decentralized Control System," *IEEJ Trans. on Industry Applications*, Vol. 126-D, No. 5, pp. 630–638, 2006.